

---

# Reinforcement Learning of Spatio-Temporal Point Processes

---

**Shixiang Zhu**

Georgia Institute of Technology  
Atlanta, GA, 30318  
shixiang.zhu@gatech.edu

**Shuang Li**

Georgia Institute of Technology  
Atlanta, GA, 30318  
sli370@gatech.edu

**Yao Xie**

Georgia Institute of Technology  
Atlanta, GA, 30318  
yao.xie@isye.gatech.edu

## Abstract

Spatio-temporal event data is ubiquitous in various applications, such as social media, crime events, and electronic health records. Spatio-temporal point processes offer a versatile framework for modeling such event data, as it can jointly capture spatial and temporal dependency. A key question is to estimate the generative model for such point processes, which enables the subsequent machine learning tasks. Existing works mainly focus on parametric models for the conditional intensity function, such as the widely used multi-dimensional Hawkes processes. However, parametric models tend to lack flexibility in tackling real data. On the other hand, non-parametric for spatio-temporal point processes tend to be less interpretable. We introduce a novel and flexible semi-parametric spatial-temporal point processes model, by combining spatial statistical models based on heterogeneous Gaussian mixture diffusion kernels, whose parameters are represented using neural networks. We learn the model using a reinforcement learning framework, where the reward function is defined via the maximum mean discrepancy (MMD) of the empirical processes generated by the model and the real data. Experiments based on real data show the superior performance of our method relative to the state-of-the-art.

## 1 Introduction

Nowadays spatio-temporal event data become ubiquitous, such as social media data, crime events, electronic health records. Such data consist of a sequence of times and locations that indicate when and where the events occurred. Modeling the dynamic generative process of the events is an important step that enables subsequent machine learning tasks. Spatio-temporal point processes offer a versatile framework for modeling the generative process of event data. In defining the generative model, a crucial step is to specify the form of the conditional intensity function, which captures the influence of past events on future events, such as self- and mutual-excitation.

However, a major challenge we face in modeling the spatio-temporal discrete data is to capture the spatial correlation between events. Take earthquake catalog data as an example. The spatial correlation between seismic activities is related to the geologic structure of faults and usually exhibits a heterogeneous conditional intensity. For instance, most aftershocks either occur along the fault plane or along other faults within the volume affected by the strain associated with the main shock. This creates a spatial profile of the intensity function that we would like to capture through the model, such as the direction and shape of the intensity function at different locations, to provide useful information to geophysicists' scientific study.

Existing literature on spatial-temporal point process modeling usually makes simplified parametric assumptions on the conditional intensity based on the prior knowledge of the processes. Landmark works [22, 21] suggest an exponential decaying kernel function. This model captures the mechanism of seismic activities to a certain degree and is easy to learn, as the kernel function is homogeneous at all locations. However, in applications to other scenarios, such parametric model may lack flexibility.

Recently, another approach to obtain generative models for point processes is based on the idea of imitation learning and reinforcement learning. Good performance has been achieved via such approach for modeling temporal processes [14] and temporal marked processes [28]. The premise is to formulate the generative model as a policy for reinforcement learning and extract policy from sequential data as if it were obtained by reinforcement learning [27] followed by inverse reinforcement learning [19, 10]. In this way, the generative model is parameterized by neural networks [3, 4, 15, 16]. However, it remains an open question on how to extend this approach to include the spatio-temporal data. The spatio-temporal point processes are significantly more challenging to model than the temporal point processes only, due to the complex spatial-temporal dependency of events.

In this paper, we present a novel model for spatio-temporal event data, by combining a spatial statistical model with point process modeling based on heterogeneous Gaussian mixture diffusion kernels, whose parameters are represented using neural networks. The advantage of our approach is that it enjoys flexible expressive power relative to the parametric model. It is also highly interpretable: using the learned functions of parameters we can understand the spatio-temporal dependency. In addition, it is computationally efficient for fitting the model to the data, since the spatial model is specified using relatively fewer number of parameters than models that are fully specified by neural networks. Our model achieves a good trade-off between model expressiveness, interpretability, and computation efficiency.

Our work improves upon existing works in the following key aspects: (1) Our work is the first to model *spatio-temporal* point processes using reinforcement learning approaches; (2) Since we built upon a spatial statistical model where neural networks are only used to represent nonlinear spatial parameters, our model is flexible and highly interpretable. For instance, the learned conditional intensity in space dimension can be used to represent the “shape of the crime” information in crime data analysis, and show how seismic activities depend on the shape of the fault zones for the earthquake catalog data. (3) We present efficient learning algorithms of our heterogeneous Gaussian mixture diffusion kernel, by coming up with an explicit formulation to connect the policy and the conditional intensity, an closed-form approximation to avoid numerical integral in the policy function, and an efficient thinning algorithm for generating samples.

Experiments on real data including robberies and earthquakes show that our method significantly outperforms the state-of-the-art. The results show that the spatial correlation learned from the data depends on the geographic features of where the events occurred. We also release an open-source implementation of our method in TensorFlow <sup>1</sup>.

Other related work using point process for related problems. Prior works such as [25, 26] have achieved some success in modeling complicated spatial pattern of crime by considering the spatial influence as *hotspots* with full parametric models. Other works [6, 34, 13, 30] consider the event sequences as temporal point processes without incorporating spatial information leverages non-parametric approaches. As a compromise, [33, 17, 15] seek to learn the spatial and temporal pattern jointly by multivariate point processes with discretized the spatial structure. There are also some other works [2, 29, 7, 4] in a similar context that serve for other purposes.

## 2 Background

In this section, we revisit the basic definitions of the spatio-temporal point processes (STPP) and the commonly used spatio-temporal diffusion kernels in STPP models.

**Spatio-temporal point processes (STPP).** STPP consists of an ordered sequence of events localized in time and location space. Let  $\{a_1, a_2, \dots, a_{N(T)}\}$  represent a sequences of points sampled from a STPP. Each point  $a_i$  is a spatio-temporal tuple  $a_i = (t_i, x_i, y_i)$ , where  $t_i \in [0, T)$  is the time of occurrence of the  $i$ -th event and  $(x_i, y_i) \in \mathcal{S} \subseteq \mathbb{R}^2$  is the associated location of the  $i$ -th event. We denote  $N(T)$  as the number of the points in the sequence between time  $[0, T)$  and in region  $\mathcal{S}$ .

---

<sup>1</sup><https://github.com/meowoodie/Spatio-Temporal-Point-Process-with-Gaussian-Mixture-Diffusion-Kernel>

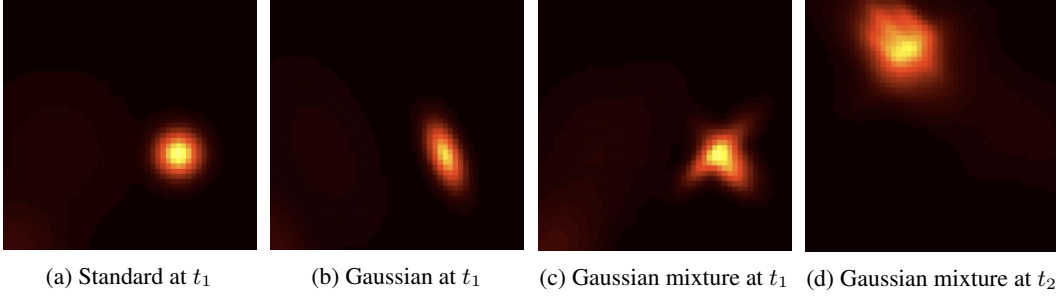


Figure 1: Conditional intensity  $\lambda^*(t, \cdot, \cdot)$  over the space  $\mathcal{S} = [-1, 1] \times [-1, 1]$ : (1a), (1b), (1c) at  $t_1 = 3.64$ , an event is occurred at  $x = 0.670, y = -0.258$  with standard defined by (2), Gaussian defined by (4), and heterogeneous Gaussian mixture defined by (3), respectively; (1d) at  $t_2 = 8.85$ , another event is occurred at  $x = -0.412, y = 0.831$ .

We characterize the event points' behaviors of a STPP using a conditional intensity function  $\lambda(t, x, y | \mathcal{H}_t)$ , which is the probability of observing an event in the spatio-temporal space  $[0, T] \times \mathcal{S}$  given the events' history  $\mathcal{H}_t = \{a_i = (t_i, x_i, y_i) | t_i < t\}$ , i.e.,

$$\lambda(t, x, y | \mathcal{H}_t) dt dx dy = \mathbb{P} \{a_{n+1} \in [t, t + dt] \times [x, x + dx] \times [y, y + dy] | \mathcal{H}_t\}.$$

In the following, we denote the above conditional intensity as  $\lambda^*(t, x, y)$  for notational simplicity.

**Hawkes model and its diffusion kernel.** According to the previous studies [21, 22, 33, 6, 13, 34] on various spatio-temporal applications, the occurrence of these events at time  $t$  depends on the historical events (before  $t$ ). To explicitly capture such dependence, Hawkes process [21] models the influence due to the past events is additive. As far as stationarity is assumed, the conditional intensity function for the spatio-temporal Hawkes model [24] is defined as

$$\lambda^*(t, x, y) = \mu + \sum_{j:t_j < t} \nu(t, t_j, x, x_j, y, y_j), \quad (1)$$

where  $\mu > 0$  is a constant background rate of event,  $\nu$  is the kernel function captures the influence of the past events. The form of the kernel function  $\nu$  determines the profile of the spatio-temporal dependency of events.

Probably the most commonly used kernel function is the standard *diffusion kernel* function proposed for the Epidemic Type Aftershock-Sequences (ETAS) modeling [18]. It was originally introduced to model the earthquake events, but now used in many other context as well. The influence of the past events decays exponentially over the spatio-temporal space (Figure 1a), and the kernel function is defined as

$$\nu(t, t_j, x, x_j, y, y_j) = \frac{C e^{-\beta(t-t_j)}}{2\pi\sigma_x\sigma_y(t-t_j)} \cdot \exp \left\{ -\frac{1}{2(t-t_j)} \left( \frac{(x-x_j)^2}{\sigma_x^2} + \frac{(y-y_j)^2}{\sigma_y^2} \right) \right\}, \quad (2)$$

where  $C$  is a constant, parameters  $\sigma_x, \sigma_y$  control the shape of the elliptical diffusion.

### 3 Proposed model

To capture complex spatial dependency with interpretable form, we present a novel kernel function motivated by the standard diffusion kernel defined by (2).

**Heterogeneous Gaussian mixture diffusion kernel.** To enhance the spatial expressiveness, we propose the heterogeneous Gaussian mixture diffusion kernel, which consists of a mixture of (extended) Gaussian diffusion kernels at each location. We also introduce additional parameters  $\rho, \mu_x, \mu_y$  to each Gaussian component to allow a continuously variable rotating and shifting of the elliptical diffusion (Figure 1b); However, to capture complex spatial dependency, we represent the parameters of the Gaussian components (defined by (4)) using neural networks. Formally, the Gaussian mixture diffusion kernel is defined as:

$$\nu(t, t_j, x, x_j, y, y_j) = \sum_{k=1}^K \phi_k \cdot g(t, t_j, x, x_j, y, y_j | \sigma_x^{(k)}, \sigma_y^{(k)}, \rho^{(k)}, \mu_x^{(k)}, \mu_y^{(k)}), \quad (3)$$

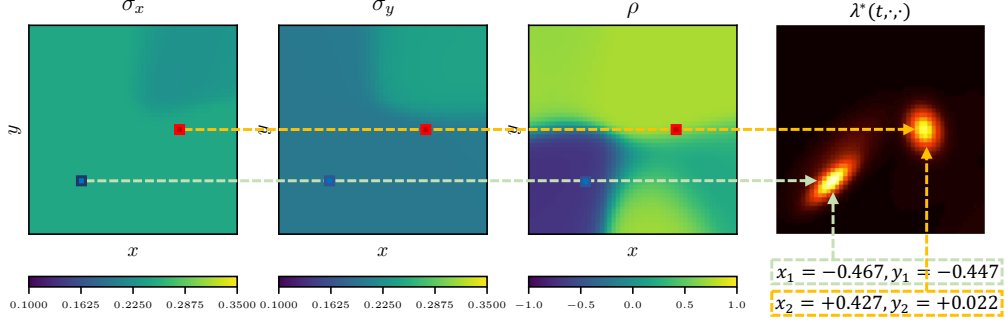


Figure 2: An example of nonlinear functions  $\sigma_x, \sigma_y, \rho$  for a heterogeneous Gaussian diffusion kernel. The right hand side is the conditional intensity at time  $t$ , where two points occurred at location  $(x_1, y_1)$  and  $(x_2, y_2)$  have triggered the two diffusions (the bright spots) with different shapes.

where  $K$  is the hyper-parameter that defines the number of components of the Gaussian mixture. The parameter  $\phi_k$  is the weight of the  $k$ -th Gaussian component which satisfies  $\sum_{k=1}^K \phi_k = 1$ . The set of parameters  $\{\sigma_x^{(k)}, \sigma_y^{(k)}, \mu_x^{(k)}, \mu_y^{(k)}, \rho^{(k)}\}$  controls the rotation, shift, and shape of the  $k$ -th Gaussian component  $g(t, t_j, x, x_j, y, y_j)$ . The Gaussian component of the kernel function is defined as:

$$g(t, t_j, x, x_j, y, y_j | \sigma_x, \sigma_y, \mu_x, \mu_y, \rho) = \frac{C \cdot e^{-\beta(t-t_j)}}{2\pi\sigma_x(x_j, y_j)\sigma_y(x_j, y_j)\sqrt{1-\rho(x_j, y_j)^2}(t-t_j)} \exp \left\{ - \left( \frac{(x-x_j-\mu_x)^2}{\sigma_x(x_j, y_j)^2} - \frac{2\rho(x_j, y_j)(x-x_j-\mu_x)(y-y_j-\mu_y)}{\sigma_x(x_j, y_j)\sigma_y(x_j, y_j)} + \frac{(y-y_j-\mu_y)^2}{\sigma_y(x_j, y_j)^2} \right) / (2(t-t_j)(1-\rho(x_j, y_j)^2)) \right\}, \quad (4)$$

where  $\sigma_x : \mathcal{S} \rightarrow \mathbb{R}^+$ ,  $\sigma_y : \mathcal{S} \rightarrow \mathbb{R}^+$ ,  $\rho : \mathcal{S} \rightarrow (-1, 1)$ ,  $\mu_x : \mathcal{S} \rightarrow \mathbb{R}$ ,  $\mu_y : \mathcal{S} \rightarrow \mathbb{R}$  are the non-linear functions that map location space to the parameters space. As shown in Figure 2, at a specific location  $(x, y)$ , parameters  $\sigma_x(x, y), \sigma_y(x, y), \rho(x, y)$  jointly control the shape and rotation of the spatial diffusion, and  $\mu_x(x, y), \mu_y(x, y)$  are the offset of the center of the diffusion kernel with respect to the location  $(x, y)$ . Figure 1 shows how conditional intensities distribute over the location space equipped with three different kernel functions.

**Neural network representation.** Recall that the spatial parameters of the diffusion are determined by a set of non-linear functions  $\{\sigma_x, \sigma_y, \mu_x, \mu_y, \rho\}$ . We adopt neural networks with a single hidden layer to capture those non-linear spatial dependencies, where the architecture is summarized in Figure 3. More specifically,

$$\begin{aligned} \sigma_x^{(k)}(x, y) &= C_0 \cdot \text{sigm}([x \ y]^T \mathbf{w}^{(k)} + b_{\sigma_x}^{(k)}), & \mu_x^{(k)}(x, y) &= C_2 \cdot (\text{sigm}([x \ y]^T \mathbf{w}^{(k)} + b_{\mu_x}^{(k)}) - 1/2), \\ \sigma_y^{(k)}(x, y) &= C_1 \cdot \text{sigm}([x \ y]^T \mathbf{w}^{(k)} + b_{\sigma_y}^{(k)}), & \mu_y^{(k)}(x, y) &= C_3 \cdot (\text{sigm}([x \ y]^T \mathbf{w}^{(k)} + b_{\mu_y}^{(k)}) - 1/2), \\ \phi_k(x, y) &= e^{[x \ y]^T \mathbf{w}_\phi^{(k)}} / \sum_{i=1}^K e^{[x \ y]^T \mathbf{w}_\phi^{(i)}}, & \rho^{(k)}(x, y) &= 2 \cdot \text{sigm}([x \ y]^T \mathbf{w}^{(k)} + b_\rho^{(k)}) - 1, \end{aligned}$$

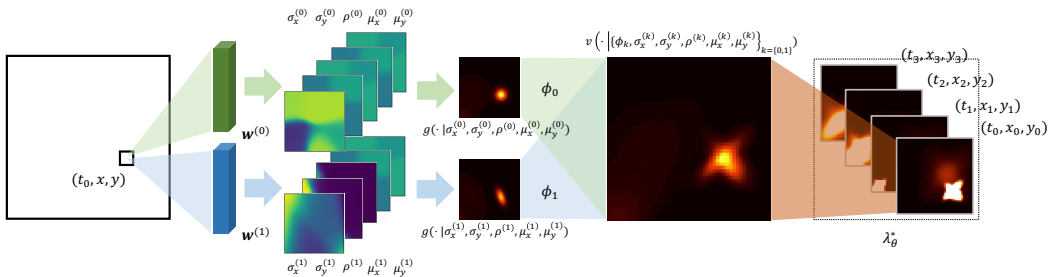


Figure 3: An illustration for the architecture of heterogeneous Gaussian mixture diffusion kernel.

where  $\text{sigm}(\cdot)$  is the sigmoid activation,  $C_0, C_1, C_2, C_3$  are constants that scale the parameters to the appropriate ranges according to the actual needs. In summary, the heterogeneous Gaussian mixture diffusion kernel is jointly parameterized by  $\theta = (\mu, \beta, \{\mathbf{w}^{(k)}, \mathbf{w}_\phi^{(k)}, b_{\sigma_x}^{(k)}, b_{\sigma_y}^{(k)}, b_\rho^{(k)}, b_{\mu_x}^{(k)}, b_{\mu_y}^{(k)}\}_{k=1\dots K})$ . By substituting (3) into (1), we obtain the semi-parametric conditional intensity function  $\lambda_\theta^*(t, x, y)$ .

## 4 Learning the proposed model

In this section, we define a reinforcement learning framework for STPP model using a policy parameterized by the conditional intensity and a non-parametric reward function based on the maximum mean discrepancy (MMD) metric.

### 4.1 Generative reinforcement learning framework

Consider the following reinforcement learning framework. A learner takes actions  $(t, x, y) \in [0, T] \times \mathcal{S}$  sequentially in an environment and the environment gives feedbacks to the learner via observing the discrepancy between the learner actions and the demonstrations provided by an expert. In our setting, both the learner actions and the demonstrations are asynchronous stochastic events localized in time and location. The learner policy  $\pi_\theta$  is parameterized by  $\theta$ . The form of  $\pi_\theta$  will be specified in Section 4.2. Assume the training data is generated by an expert policy  $\pi_\mathcal{E}$ , where the subscript  $\mathcal{E}$  denotes ‘‘expert’’. Let  $\mathcal{A} = \{\alpha_j\}, j = 1, 2, \dots, N$  be the trajectories generated by the learner  $\pi_\theta$ , where each  $\alpha_j = \{a_0, a_1, \dots, a_{N_{\alpha_j}}\}$  denotes a single action trajectory with length  $N_{\alpha_j}$ . We will discuss how to generate samples from our model in Section 4.4. Let  $\mathcal{E} = \{\epsilon_j\}, j = 1, 2, \dots, M$  be the demonstrations provided by the expert  $\pi_\mathcal{E}$ , where each  $\epsilon_j = \{e_0, e_1, \dots, e_{N_{\epsilon_j}}\}$  denotes a single demonstration with length  $N_{\epsilon_j}$ . The goal is to find the optimal policy that maximize the expected reward evaluated by a reward function  $r_{\mathcal{A}, \mathcal{E}}(\cdot)$ ,

$$\underset{\theta}{\text{maximize}} \quad \mathbb{E}_{\alpha \sim \pi_\theta, \epsilon \sim \pi_\mathcal{E}} \left[ \sum_{i=1}^{N_\alpha} r_{\mathcal{A}, \mathcal{E}}(a_i) \right], \quad (5)$$

where  $\alpha = \{a_1, \dots, a_{N_\alpha}\}$  is one sampled roll-out from policy  $\pi_\theta$ . Note that  $N_\alpha$  can be different for different roll-out samples. The reward function  $r_{\mathcal{A}, \mathcal{E}}$  measures the discrepancy between the distribution of the observed training data and the distribution of the actions, which we will discuss in Section 4.3. The expectation is taken over all possible realizations of the STPP associated with the learner’s action trajectories and the expert’s demonstrations. In Appendix B, Figure 5 illustrates of the reinforcement learning framework.

### 4.2 Policy parameterization

We parameterize the learner policy using STPP with the proposed heterogeneous Gaussian mixture diffusion kernel in Section 3. The learner policy is denoted as  $\pi_\theta(a)$ , where  $a = (t, x, y)$  is a 3-dimensional vector specifying the possible time and location of the action given the history. We show that the policy  $\pi_\theta(a)$  is related to the conditional probability density explicitly. This connection is crucial in linking the point process model and the reinforcement learning framework.

**Lemma 1.** *Consider the policy  $\pi_\theta(t, x, y)$  of a STPP for any  $t > t_n$ , the conditional intensity function is defined by*

$$\lambda_\theta^*(t, x, y) = \frac{\pi_\theta(t, x, y)}{1 - \int_0^t \int_{\mathcal{S}} \pi_\theta(\tau, u, v) d\tau dudv}.$$

The proof is shown in Appendix A, using arguments similar to those in [23].

Using the above lemma, we can specify the form of the policy explicitly. Let  $F^*(t) = \mathbb{P}\{t_{n+1} < t | \mathcal{H}_t\} = \int_0^t \int_{\mathcal{S}} \pi_\theta(\tau, u, v) d\tau dudv$  be the conditional probability that next event  $t_{n+1}$  happens in region  $\mathcal{S}$  before  $t$  given the history. From the above lemma, we obtain  $\int_{\mathcal{S}} \lambda_\theta^*(t, u, v) dudv = \frac{d}{dt} F^*(t) / (1 - F^*(t)) = -\frac{d}{dt} \log(1 - F^*(t))$ . Hence,  $\int_{t_n}^t \int_{\mathcal{S}} \lambda_\theta^*(\tau, u, v) d\tau dudv = -\log(1 - F^*(t))$ , where  $F^*(t_n) = 0$  since event  $n + 1$  does not exist at time  $t_n$ . Therefore, we obtain the learner policy as the following proposition:

**Proposition 1.** *Given the conditional intensity function  $\lambda_\theta^*(t, x, y)$ , the learner policy of a STPP on  $[0, T] \times \mathcal{S}$  is given by*

$$\pi_\theta(t, x, y) = \lambda_\theta^*(t, x, y) \cdot \exp \left\{ - \int_{t_n}^t \int_{\mathcal{S}} \lambda_\theta^*(\tau, u, v) d\tau dudv \right\}. \quad (6)$$

A crucial step to tackle the computational challenge is to evaluate the integral in (6). Due to the decreased activity in the marginal and outer part of the region, the boundary effect in the policy function and likelihood calculation is usually negligible [22]. Thus, we can approximate the integral term in (6) by analytically integrating over  $\mathbb{R}^2$  instead of an arbitrary  $\mathcal{S}$ . Using the approximation  $\int_{t_n}^t \int_{\mathcal{S}} \lambda_{\theta}^*(t, x, y) dt dx dy \leq \int_{t_n}^t \int_{\mathbb{R}^2} \lambda_{\theta}^*(t, x, y) dt dx dy$  can reduce the integral to an analytical form which can be evaluated directly without numerical integral. The proof of the Proposition 2 is shown in Appendix C.

**Proposition 2.** *Given the conditional intensity function  $\lambda_{\theta}^*(t, x, y)$  with heterogeneous Gaussian mixture diffusion kernel defined by (3), the learner policy of a STPP on  $[0, T) \times \mathcal{S}$  is approximately*

$$\pi_{\theta}(t, x, y) \approx \lambda_{\theta}^*(t, x, y) \cdot \exp \left\{ -\mu(t - t_n)|\mathcal{S}| - \sum_{i:t_i < t} \frac{C}{\beta} \left( e^{-\beta(t_n - t_i)} - e^{-\beta(t - t_i)} \right) \right\},$$

where  $|\mathcal{S}|$  is the area of the region  $\mathcal{S}$ .

### 4.3 Reward function

We need to evaluate the discrepancy between the empirical distribution of the data, and the distribution of the sequence generated from the algorithm. In this setting, the distributional form of the joint distribution of the sequence of events is hard to specify analytically (since they are stochastic processes with complex spatial and temporal dependency). Maximum mean discrepancy (MMD) is a natural choice and it is non-parametric.

We generalized the idea of MMD reward in [11, 9, 5, 14] from a simple one-dimensional temporal point process to the spatio-temporal setting. Given the expert policy  $\pi_{\mathcal{E}}$ , the optimal reward function  $\hat{r}_{\mathcal{A}, \mathcal{E}}$  can be uncovered by solving the inverse reinforcement learning problem:

$$\hat{r}_{\mathcal{A}, \mathcal{E}} = \arg \max_{r_{\mathcal{A}, \mathcal{E}} \in \mathcal{F}} \left( \mathbb{E}_{\epsilon \sim \pi_{\mathcal{E}}} \left[ \sum_{i=1}^{N_{\epsilon}} r_{\mathcal{A}, \mathcal{E}}(e_i) \right] - \max_{\pi_{\theta} \in \mathcal{G}} \mathbb{E}_{\alpha \sim \pi_{\theta}} \left[ \sum_{i=1}^{N_{\alpha}} r_{\mathcal{A}, \mathcal{E}}(a_i) \right] \right), \quad (7)$$

where  $\mathcal{G}$  is the family of all candidate policies  $\pi_{\theta}$  and  $\mathcal{F}$  is the family class for reward function  $r_{\mathcal{A}, \mathcal{E}}$  in reproducing kernel Hilbert space (RKHS). The formulation means that a proper reward function should give the expert policy higher reward than any other learner policy in  $\mathcal{G}$ . Thus the learner can approach the expert performance by maximizing this reward.

According to Theorem 1 in [14], we obtain analytical expression to the inverse reinforcement learning problem (7). A finite sample estimate of the optimal reward is as follows. Given  $L$  learner trajectories generated by  $\pi_{\theta}$ , and  $M$  expert sequences generated by  $\pi_{\mathcal{E}}$ , mean embeddings  $\mu_{\pi_{\theta}}$  and  $\mu_{\pi_{\mathcal{E}}}$  can be estimated by their respective empirical means:

$$\mu_{\pi_{\theta}} = \frac{1}{L} \sum_{l=1}^L \sum_{i=1}^{N_{\alpha_l}^{(l)}} k(a_i^{(l)}, \cdot), \quad \text{and} \quad \mu_{\pi_{\mathcal{E}}} = \frac{1}{M} \sum_{m=1}^M \sum_{i=1}^{N_{\epsilon_m}^{(m)}} k(e_i^{(m)}, \cdot),$$

where  $k(\cdot, \cdot)$  is a reproducing kernel Hilbert space (RKHS) kernel. Here we use Gaussian kernel function. For any  $t \in [0, T)$ , the estimated optimal reward is

$$\hat{r}_{\mathcal{A}, \mathcal{E}}(a) \propto \frac{1}{L} \sum_{l=1}^L \sum_{i=1}^{N_{\alpha_l}^{(l)}} k(a_i^{(l)}, a) - \frac{1}{M} \sum_{m=1}^M \sum_{i=1}^{N_{\epsilon_m}^{(m)}} k(e_i^{(m)}, a). \quad (8)$$

Equipped with the optimal reward in (5), the gradient of the policy  $\nabla_{\theta} J(\theta)$  can be estimated by using *policy gradient*, as shown in Appendix D. The learning algorithm for our model is summarized in Algorithm 1.

### 4.4 Efficient thinning algorithm for drawing samples from STPP

To generate samples from our proposed model, *i.e.*,  $a \sim \pi_{\theta}$ , given the history  $\mathcal{H}_t$ , we need to sample a point tuple  $a = (t, x, y)$  according to the conditional intensity defined by (1). A default way to simulate point processes is to use thinning algorithm [8, 1]. However, the vanilla thinning algorithm suffers from low sampling efficiency as it needs to sample in the space  $|\mathcal{S}| \times [0, T)$  uniformly with the upper limit of the conditional intensity  $\bar{\lambda}$  and only very few of candidate points will be retained in the end. In particular, given the parameter  $\theta$ , the computing complexity of the procedure increases exponentially with the size of the sampling space.

To improve sampling efficiency, we propose an efficient thinning algorithm summarized in Algorithm 2, Appendix E. The “proposal” density is a non-homogeneous STPP, whose intensity function is defined from the previous iterations. This is analogous to the idea of importance sampling [20]. Let  $\alpha$  represent the ordered set of accepted points,  $(t_n, x_n, y_n)$  be the latest accepted point, and  $t$  be the time when the newest candidate point is generated. We can guarantee that  $\lambda = \mu + \sum_{(\tau, u, v) \in \alpha} \nu(t, \tau, x_n, u, y_n, v) > \lambda_\theta^*(t + w, x, y), \forall w > 0, (x, y) \in \mathcal{S}$  if  $\mu_x(x, y), \mu_y(x, y)$  are sufficiently small relative to  $\sigma_x(x, y), \sigma_y(x, y)$ , which leads to the updating rule for  $\bar{\lambda}$ .

---

**Algorithm 1:** Reinforcement learning for learning STPP

---

Initialize the model parameter  $\theta$  for the model  $\lambda_\theta^*, \pi_\theta$ ; set  $N$  as the number of batches and let  $n = 0$ ;  
**while**  $n < N$  **do**

Sample  $M$  demonstrations  $\{\epsilon_0, \dots, \epsilon_M\}$  from the expert  $\pi_\epsilon$  where  $\epsilon_m = \{e_0^{(m)}, \dots, e_{N_{\epsilon_m}}^{(m)}\}$ ;  
 Sample  $L$  actions  $\{\alpha_0, \dots, \alpha_L\}$  by performing Algorithm 2 according to  $\lambda_\theta^*$ , where  
 $\alpha_l = \{a_0^{(l)}, \dots, a_{N_{\alpha_l}}^{(l)}\}$ ;  
 Given arbitrary action  $a$ , the optimal reward is estimated by  
 $\hat{r}_{\mathcal{A}, \mathcal{E}}(a) = \frac{1}{L} \sum_{l=1}^L \sum_{i=1}^{N_{\alpha_l}^{(l)}} k(a_i^{(l)}, a) - \frac{1}{M} \sum_{m=1}^M \sum_{i=1}^{N_{\epsilon_m}^{(m)}} k(e_i^{(m)}, a)$ ;  
 Estimate policy gradient  $\nabla_\theta J(\theta) \approx \frac{1}{L} \sum_{j=1}^L \left[ \sum_{i=1}^{N_{\alpha_j}} (\nabla_\theta \log \pi_\theta(a_i) \cdot \hat{r}_{\mathcal{A}, \mathcal{E}}(a_i)) \right]$ ;  
 Update model parameters as  $\theta \leftarrow \theta + \gamma \nabla_\theta J(\theta)$  where  $\gamma$  is the learning rate;  
 $n \leftarrow n + 1$ .

**end**

---

## 5 Experimental results

In this section, we compare our proposed **Hawkes process with heterogeneous Gaussian mixture diffusion kernel (H-HGMD)** with benchmarks and the state-of-the-art in the field, including (1) **Random uniform** that randomly makes actions in the action space; (2) **Hawkes type ETAS (H-ETAS)** with standard diffusion kernel, which is currently the most widely used approach in spatial-temporal event data modeling. For H-ETAS, the parameters are estimated by maximum likelihood estimate (MLE); (3) **H-HGMD+RL** is our approach using the reinforcement learning; (4) **H-HGMD+MLE** is our approach where the parameters are estimated by MLE, as explained in Appendix G; (5) **reinforcement learning point processes model (RLPP)** [14] is for modeling temporal point process only, which cannot be easily generalized to spatio-temporal models.

Table 1: Comparison of MMD between simulated and training sequences.

	Random uniform	H-ETAS	H-HGMD + RL	H-HGMD + MLE	RLPP
Robbery (space-time)	108.004	72.869	68.372	69.372	N/A
Seismic (space-time)	53.139	32.185	21.147	28.622	N/A
Robbery (time only)	126.782	90.607	82.189	83.750	83.134
Seismic (time only)	60.725	51.037	21.223	27.256	17.251

**Performance metrics.** To evaluate the performance of algorithms (*i.e.*, various generative models), we use MMD metric between the real observed sequences and the generated sequences from the models, as specified in Section 4.3.

We test our approach on two real datasets that contain complex spatial dependency. Such dependency is highly related to geographic features:

**Atlanta 911 calls-for-service data.** The 911 calls-for-service data in Atlanta from the end of 2015 to the middle of 2017 is provided by the Atlanta Police Department. This dataset has been previously used to validate the crime linkage detection algorithm [31, 32, 33]. We extract 7,831 reported robbery from the dataset since robbers usually follow particular *modus operandi* (M.O.) where criminal spots and times tend to have a causal relationship with each other. Then we partition the sequence into pieces by month. Each robbery report is associated with the time (accurate to the second) and the geolocation (latitude and longitude) indicating when and where the robbery occurred.

**Northern California seismic data.** The Northern California Earthquake Data Center (NCEDC) provides public time series data [12] that comes from broadband, short period, strong motion seismic sensors, and GPS, and other geophysical sensors. We extract 16,401 seismic records that have magnitude larger than 3.0 from 1978 to 2018 in Northern California and partition the sequence into



smaller pieces on a quarterly basis. For the purpose of testing our model, each record only contains time and geolocation.

We quantitatively compare the methods by calculating the average absolute MMD values between the observed training data and the generated sequences. The absolute value of MMD indicates the level of similarity of two arbitrary distributions. If two distributions are exactly the same, then their absolute MMD value is zero. In the experiment, we randomly pick 100 pairs of generated sequences against observed sequences from the real datasets and compute their average absolute MMD value. As shown in Table 1, our approaches are highlighted with the **red columns**, complete space-time datasets are highlighted with the **green rows**, and the **orange cells** highlight the results our models obtained. According to the MMD values, our methods H-HGMD + RL and H-HGMD + MLE outperforms the state-of-the-art (H-ETAS). In addition, we also show that our method has competitive performance only in terms of the temporal correlation comparing to RLPP which is only able to produce the temporal sequences.

To interpret the spatial dependency learned using our model, we visualize the conditional intensity at certain times on the map. Regarding the state-of-the-art, as shown in Figure 4c, 4f, we can see that the H-ETAS only learned the distribution of base conditional intensity. However, it fails to capture the differences of spatial pattern between different types of event and the edge detail of spatial pattern for each of events. Any event from the same sequence produces diffusion with the same shape no matter where and when it occurred.

Comparing our results with the state-of-the-art, we can see a major difference is: the characteristics of different types of events make the event spread its spatial influence in various ways. Regarding 911 calls-for-service data, as shown in Figure 4b, 4a, the spatial influence of some newly occurred robbery events washes to the surrounding streets and the community blocks unevenly. For seismic data, in Figure 4e, 4d, 4f, the principal spatial influence of an event is basically disseminated along the earthquake fault lines. Appendix F gives a concrete example of the robbery sequences.

## 6 Conclusion

We proposed a new semi-parametric generative model for spatio-temporal event data by combining spatial statistical models with reinforcement learning. The spatio-temporal point processes are represented as a Hawkes model whose conditional intensity is represented using heterogeneous Gaussian mixture diffusion kernel. The three parameters of each Gaussian components is parameterized by neural networks; so there are relatively to a full neural network model. This model leads to a statistical part that is highly interpretation. We also proposed efficient learning algorithms for learning such model from data based on reinforcement learning, where the reward function is estimated using maximum mean discrepancy (MMD) metric (therefore completely data-driven), and the optimal

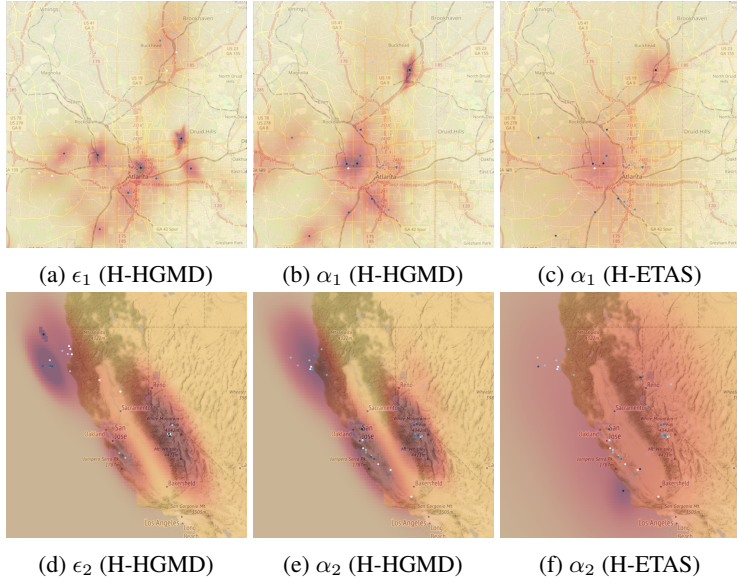


Figure 4: **Top row**: the conditional intensity of robberies in Atlanta at time  $t$ . **Bottom row**: the conditional intensity of earthquakes in North of California at time  $t$ .  $\alpha_1, \alpha_2$  are two sequences generated by the fitted models and  $\epsilon_1, \epsilon_2$  are two training sequences. Models are fitted by (4b, 4a, 4e, 4d) RL with heterogeneous Gaussian mixture diffusion kernel ( $K = 5$ ), and (4f, 4c) Hawkes type ETAS, respectively. The dots on the maps are the occurred events in which dark blue represents the newly happened events, and white represents events happened close to  $t$ .



policy is related to our conditional intensity in closed-form. Experiments show that our model is capable in capturing the spatio-temporal pattern adaptively for different types of data and achieve competitive performance relative to the state-of-the-art. Ongoing future work involves applying the generative model for anomaly detection for spatial temporal event data, as well as generalize our method for spatio-temporal marked point processes.

## References

- [1] D. J. Daley and D. Vere-Jones. *An introduction to the theory of point processes. Vol. II.* Probability and its Applications (New York). Springer, New York, second edition, 2008. General theory and structure.
- [2] Kenji Doya. Reinforcement learning in continuous time and space. *Neural Computation*, 12(1):219–245, 2000.
- [3] Nan Du, Hanjun Dai, Rakshit Trivedi, Utkarsh Upadhyay, Manuel Gomez-Rodriguez, and Le Song. Recurrent marked temporal point processes: Embedding event history to vector. In *Proceedings of the 22Nd ACM SIGKDD International Conference on Knowledge Discovery and Data Mining*, KDD '16, pages 1555–1564, New York, NY, USA, 2016. ACM.
- [4] Yan Duan, Xi Chen, Rein Houthoofd, John Schulman, and Pieter Abbeel. Benchmarking deep reinforcement learning for continuous control. In *Proceedings of the 33rd International Conference on International Conference on Machine Learning - Volume 48*, ICML'16, pages 1329–1338. JMLR.org, 2016.
- [5] Gintare Karolina Dziugaite, Daniel M. Roy, and Zoubin Ghahramani. Training generative neural networks via maximum mean discrepancy optimization. In *Proceedings of the Thirty-First Conference on Uncertainty in Artificial Intelligence*, UAI'15, pages 258–267, Arlington, Virginia, United States, 2015. AUAI Press.
- [6] Eric W. Fox, Martin B. Short, Frederic P. Schoenberg, Kathryn D. Coronges, and Andrea L. Bertozzi. Modeling e-mail networks and inferring leadership using self-exciting point processes. *Journal of the American Statistical Association*, 111(514):564–584, 2016.
- [7] N. Frémaux, H. Sprekeler, and W. Gerstner. Reinforcement Learning Using a Continuous Time Actor-Critic Framework with Spiking Neurons. *PLoS Computational Biology*, 9:e1003024, April 2013.
- [8] Edith Gabriel, Barry Rowlingson, and Peter Diggle. stpp: An r package for plotting, simulating and analyzing spatio-temporal point patterns. *Journal of Statistical Software*, 53:1–29, 04 2013.
- [9] Arthur Gretton, Karsten Borgwardt, Malte Rasch, Bernhard Schölkopf, and Alex J. Smola. A kernel method for the two-sample-problem. In *Advances in Neural Information Processing Systems 19*, pages 513–520. MIT Press, 2007.
- [10] Jonathan Ho and Stefano Ermon. Generative adversarial imitation learning. In D. D. Lee, M. Sugiyama, U. V. Luxburg, I. Guyon, and R. Garnett, editors, *Advances in Neural Information Processing Systems 29*, pages 4565–4573. Curran Associates, Inc., 2016.
- [11] Beomjoon Kim and Joelle Pineau. Maximum mean discrepancy imitation learning. In *Robotics: Science and Systems*, 2013.
- [12] Northern California Earthquake Data Center. UC Berkeley Seismological Laboratory. NCEDC, 2014.
- [13] Erik Lewis, George Mohler, P Jeffrey Brantingham, and Andrea L Bertozzi. Self-exciting point process models of civilian deaths in iraq. *Security Journal*, 25(3):244–264, Jul 2012.
- [14] Shuang Li, Shuai Xiao, Shixiang Zhu, Nan Du, Yao Xie, and Le Song. Learning temporal point processes via reinforcement learning. In *Advances in Neural Information Processing Systems 31*, pages 10781–10791. Curran Associates, Inc., 2018.
- [15] Hongyuan Mei and Jason Eisner. The neural hawkes process: A neurally self-modulating multivariate point process. In *Proceedings of the 31st International Conference on Neural Information Processing Systems*, NIPS'17, pages 6757–6767, USA, 2017. Curran Associates Inc.

- [16] Volodymyr Mnih, Adria Puigdomenech Badia, Mehdi Mirza, Alex Graves, Timothy Lillicrap, Tim Harley, David Silver, and Koray Kavukcuoglu. Asynchronous methods for deep reinforcement learning. In Maria Florina Balcan and Kilian Q. Weinberger, editors, *Proceedings of The 33rd International Conference on Machine Learning*, volume 48 of *Proceedings of Machine Learning Research*, pages 1928–1937, New York, New York, USA, 20–22 Jun 2016. PMLR.
- [17] G. O. Mohler, M. B. Short, P. J. Brantingham, F. P. Schoenberg, and G. E. Tita. Self-exciting point process modeling of crime. *Journal of the American Statistical Association*, 106(493):100–108, 2011.
- [18] F. Musmeci and D. Vere-Jones. A space-time clustering model for historical earthquakes. *Annals of the Institute of Statistical Mathematics*, 44(1):1–11, Mar 1992.
- [19] Andrew Y. Ng and Stuart Russell. Algorithms for inverse reinforcement learning. In *in Proc. 17th International Conf. on Machine Learning*, pages 663–670. Morgan Kaufmann, 2000.
- [20] Yosihiko Ogata. On lewis’ simulation method for point processes. *IEEE Transactions on Information Theory*, 27(1):23–31, January 1981.
- [21] Yosihiko Ogata. Statistical models for earthquake occurrences and residual analysis for point processes. *Journal of the American Statistical Association*, 83(401):9–27, 1988.
- [22] Yosihiko Ogata. Space-time point-process models for earthquake occurrences. *Annals of the Institute of Statistical Mathematics*, 50(2):379–402, 1998.
- [23] Jakob Gulddahl Rasmussen. Temporal point processes: the conditional intensity function, Jan 2011.
- [24] Alex Reinhart. A review of self-exciting spatio-temporal point processes and their applications. *Statist. Sci.*, 33(3):299–318, 08 2018.
- [25] M. Short, A. Bertozzi, and P. Brantingham. Nonlinear patterns in urban crime: Hotspots, bifurcations, and suppression. *SIAM Journal on Applied Dynamical Systems*, 9(2):462–483, 2010.
- [26] Martin B. Short, P. Jeffrey Brantingham, Andrea L. Bertozzi, and George E. Tita. Dissipation and displacement of hotspots in reaction-diffusion models of crime. *Proceedings of the National Academy of Sciences*, 107(9):3961–3965, 2010.
- [27] Richard S Sutton and Andrew G Barto. *Reinforcement learning: An introduction*. MIT press, Cambridge, 1998.
- [28] Utkarsh Upadhyay, Abir De, and Manuel Gomez-Rodriguez. Deep reinforcement learning of marked temporal point processes. In *Advances in Neural Information Processing Systems 31*, 2018.
- [29] Eleni Vasilaki, Nicolas Frémaux, Robert Urbanczik, Walter Senn, and Wulfram Gerstner. Spike-based reinforcement learning in continuous state and action space: When policy gradient methods fail. *PLOS Computational Biology*, 5(12):1–17, 12 2009.
- [30] Shuai Xiao, Mehrdad Farajtabar, Xiaojing Ye, Junchi Yan, Le Song, and Hongyuan Zha. Wasserstein learning of deep generative point process models. In *Proceedings of the 31st International Conference on Neural Information Processing Systems, NIPS’ 17*, pages 3250–3259. Curran Associates Inc., 2017.
- [31] Shixiang Zhu and Yao Xie. Crime event embedding with unsupervised feature selection, 2018.
- [32] Shixiang Zhu and Yao Xie. Crime incidents embedding using restricted boltzmann machines. *2018 IEEE International Conference on Acoustics, Speech and Signal Processing (ICASSP)*, pages 2376–2380, 2018.
- [33] Shixiang Zhu and Yao Xie. Crime linkage detection by spatio-temporal-textual point processes, 2019.
- [34] Joseph R. Zipkin, Frederic P. Schoenberg, Kathryn Coronges, and Andrea L. Bertozzi. Point-process models of social network interactions: Parameter estimation and missing data recovery. *European Journal of Applied Mathematics*, 27(3):502–529, 2016.

## A Proof of Lemma 1

The following informal derivation justifies the lemma.

$$\begin{aligned}
& \lambda(t, x, y | \mathcal{H}_t) dt dx dy \\
&= \mathbb{E} \{ N([t, t + dt] \times [x, x + dx] \times [y, y + dy]) | \mathcal{H}_{t-} \} \\
&= \mathbb{P} \{ e_{n+1} \in [t, t + dt] \times [x, x + dx] \times [y, y + dy] | \mathcal{H}_{t-} \} \\
&= \mathbb{P} \{ e_{n+1} \in [t, t + dt] \times [x, x + dx] \times [y, y + dy] | e_{n+1} \notin (t_n, t) \times \mathcal{S}, \mathcal{H}_{t_n} \} \\
&= \frac{\mathbb{P} \{ e_{n+1} \in [t, t + dt] \times [x, x + dx] \times [y, y + dy], e_{n+1} \notin (t_n, t) \times \mathcal{S} | \mathcal{H}_{t_n} \}}{\mathbb{P} \{ e_{n+1} \notin (t_n, t) \times \mathcal{S} | \mathcal{H}_{t_n} \}} \\
&= \frac{\mathbb{P} \{ e_{n+1} \in [t, t + dt] \times [x, x + dx] \times [y, y + dy] | \mathcal{H}_{t_n} \}}{\mathbb{P} \{ e_{n+1} \notin (t_n, t) \times \mathcal{S} | \mathcal{H}_{t_n} \}} \\
&= \frac{\pi_\theta(t, x, y)}{1 - \int_0^t \int_{\mathcal{S}} \pi_\theta(\tau, u, v) d\tau dudv}.
\end{aligned}$$

where  $N(A)$  denotes the number of points falling in an interval  $A$ . Here the numerator is the learner policy according to the definition.

## B Reinforcement learning framework

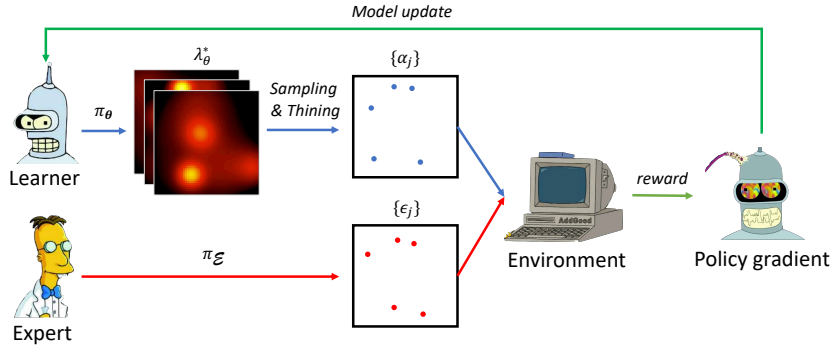


Figure 5: Illustration for the reinforcement learning framework for STPP. A learner takes actions via sampling and thinning according to the intensity function determined by the current learner policy  $\pi_\theta$ . The observed expert demonstrations are sampled from an expert policy  $\pi_\mathcal{E}$ . The environment compares the MMD between the learner actions and the expert demonstrations and update the learner policy accordingly.

## C Proof of Proposition 2

The conditional probability density is

$$\pi_\theta(t, x, y) = \lambda_\theta^*(t, x, y) \exp \left\{ - \int_{t_n}^t \int_{\mathcal{S}} \lambda_\theta^*(\tau, u, v) d\tau dudv \right\}$$

where  $\theta = (\mu, \beta, \{\mathbf{w}^{(k)}, \mathbf{w}_\phi^{(k)}, b_{\sigma_x}^{(k)}, b_{\sigma_y}^{(k)}, b_\rho^{(k)}, b_{\mu_x}^{(k)}, b_{\mu_y}^{(k)}\}_{k=1 \dots K})$  is the parameters of the point process. The integral part can be done by

$$\begin{aligned}
& \int_{t_n}^t \int_{\mathcal{S}} \lambda_\theta^*(\tau, u, v) d\tau dudv \\
&= \int_{t_n}^t \int_{\mathcal{S}} \left[ \mu + \sum_{i:t_i < \tau} \sum_{k=1}^K \phi_k \cdot g(\tau, t_i, u, x_i, v, y_i | \theta_{-\mu}) \right] d\tau dudv \\
&\approx \mu(t - t_n) |\mathcal{S}| + \sum_{k=1}^K \phi_k \sum_{i:t_i < \tau} \int_{t_n}^t \int_{\mathbb{R}^2} g(\tau, t_i, u, x_i, v, y_i | \theta_{-\mu}) d\tau dudv
\end{aligned}$$

where  $|\mathcal{S}|$  is the area of the space region. The triple integral in the second term can be written explicitly by changing variable. Let  $r$  be the radius of the ellipse,  $\psi$  be the angle, so that we have  $u/\sigma_x = r \cos(\psi)$ ,  $v/\sigma_y = r \sin(\psi)$ . Therefore, the triple integral, which is independent from  $r$  and  $\psi$ , can be written as

$$\begin{aligned} & \int_{t_n}^t \int_{\mathbb{R}^2} g(\tau, t_i, u, x_i, v, y_i | \theta_{-\mu}) d\tau du dv \\ &= \int_{t_n}^t \int_0^{2\pi} \int_0^\infty \frac{Cr}{2\pi\tau} \exp\{-\beta\tau - r^2/2\tau\} d\tau d\psi dr \\ &= \frac{C}{\beta} \left( e^{-\beta(t_n-t_i)} - e^{-\beta(t-t_i)} \right) \end{aligned}$$

Sum above equations, we can obtain the analytical form of the conditional probability density of the point processes,

$$\pi_\theta(t, x, y) \approx \lambda_\theta^*(t, x, y) \cdot \exp \left\{ -\mu(t - t_n)|\mathcal{S}| - \sum_{i:t_i < t} \frac{C}{\beta} \left( e^{-\beta(t_n-t_i)} - e^{-\beta(t-t_i)} \right) \right\}$$

## D Policy gradient

In the following, we denote the expected reward defined by (5) as  $J(\theta)$  a function of the policy parameters, where the optimal policy  $\hat{\pi}_\theta$  can be attained by maximizing the expected reward. With the likelihood ratio trick, the gradient of  $J(\theta)$  with respect to  $\theta$  can be computed by using policy gradient with variance reduction [14],

$$\begin{aligned} \nabla_\theta J(\theta) &= \mathbb{E}_{\alpha \sim \pi_\theta, \epsilon \sim \pi_\mathcal{E}} \left[ \sum_{i=1}^{N_\alpha} (\nabla_\theta \log \pi_\theta(a_i)) \cdot \sum_{i=1}^{N_\alpha} \hat{r}_{\mathcal{A}, \mathcal{E}}(a_i) \right] \\ &\approx \frac{1}{L} \sum_{j=1}^L \left[ \sum_{i=1}^{N_{\alpha_j}} (\nabla_\theta \log \pi_\theta(a_i)) \cdot \hat{r}_{\mathcal{A}, \mathcal{E}}(a_i) \right] \end{aligned} \quad (9)$$

where  $\sum_{i=1}^{N_{\alpha_j}} (\nabla_\theta \log \pi_\theta(a_i))$  is the gradient of the log-likelihood of a roll-out sample  $\alpha_j = \{a_0, a_1, \dots, a_{N_{\alpha_j}(T)}\}$ . To estimate the expected reward, we sample  $M$  sequences from the current policy, and compute the estimated gradient accordingly.

## E Efficient thinning algorithm for STPP

---

**Algorithm 2:** Efficient thinning algorithm for simulating STPP

---

**input:**  $\mu, \beta, \nu, T, \mathcal{S}$

**output:** A set of ordered points  $\alpha$

Initialize  $\alpha = \emptyset, t = 0, x, y \sim \text{uniform}(\mathcal{S}), n = 0$ ;

**while**  $t < T$  **do**

Set  $\bar{\lambda} = \mu + \sum_{(\tau, u, v) \in \alpha} \nu(t, \tau, x_n, u, y_n, v)$ ; //  $(t_n, x_n, y_n)$  is the last point in  $\alpha$

Generate  $u \sim \text{uniform}(0, 1)$ ;

Let  $w = -\ln u/\bar{\lambda}$ ; //so that  $w \sim \exp(\bar{\lambda})$

Set  $t = t + w$ ; //  $t$  is the time for the candidate point

Uniformly sample  $x, y$  from  $\mathcal{S}$ ;

Generate  $D \sim \text{uniform}(0, 1)$ ;

**if**  $D\bar{\lambda} > \lambda_\theta^*(t, x, y)$  **then**

$t_n = t, x_n = x, y_n = y$ ;

$\alpha = \alpha \cup \{(t_n, x_n, y_n)\}$ ;

$n = n + 1$ ;

//adding point to the order set  $\alpha$

**end**

**end**

---

## F Conditional intensity interpretation

In Figure 6, each subfigure shows that events at different types of the urban region have various shape of spatial influence to their surroundings. For example, the events occurred near to the highway or railroad spread their influence along the road, and the events at the midtown area have more dense influence diffusion than the events in the rural area.

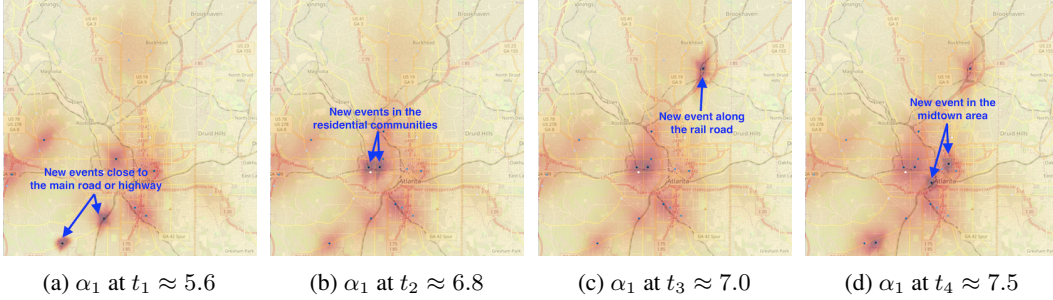


Figure 6: The conditional intensities of the robbery sequence  $\alpha_1$  over the space at moment (6a)  $t_1 \approx 5.6$ , (6b)  $t_2 \approx 6.8$ , (6c)  $t_3 \approx 7.0$ , (6d)  $t_4 \approx 7.5$ , respectively. Different robbery events at different locations in the same sequence have very distinctive pattern of spatial influence to their neighbourhood, which may be related to some geographic feature of the locations.

## G Maximum likelihood estimate

Our model is also simple as well as intuitive due to the explicit form of the intensity function, which makes it easy to estimate the parameters via maximum likelihood estimate (MLE) as illustrated in Figure 7. Assume that we have observed a point pattern  $\epsilon = \{e_0, e_1, \dots, e_{N_\epsilon}\}$  occurred on  $(0, T] \times \mathcal{S}$  with length  $N_\epsilon$ , where  $e_i = (t_i, x_i, y_i)$ . Then the likelihood is given by

$$\mathcal{L}(\theta) = \left( \prod_{i=1}^{N_\epsilon} \lambda_\theta^*(t_i, x_i, y_i) \right) \exp \left\{ - \int_0^T \int_{\mathcal{S}} \lambda_\theta^*(\tau, u, v) d\tau dudv \right\}. \quad (10)$$

The optimal model is obtained by  $\hat{\theta} = \operatorname{argmax}_\theta \log \mathcal{L}(\theta)$ . Due to the non-convex nature of this problem, the problem can be solved by stochastic gradient descent.

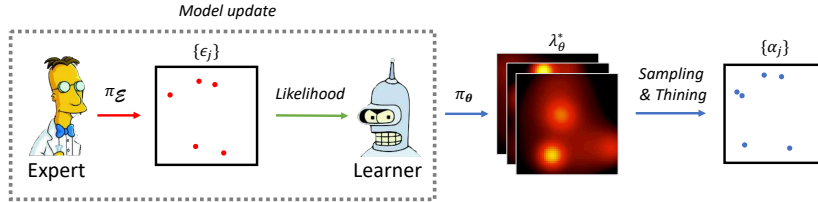


Figure 7: Illustration for the MLE framework. An expert provides training data, and update the model by maximizing the likelihood.